Composition and growth mode of MoS_x sputtered films

J. Moser and F. Lévy
Institut de Physique Appliquée, Ecole Polytechnique Fédérale de Lausanne, CH-1015 Lausanne, Switzerland

F. Bussy
Institut de Minéralogie, BFSH 2, Université de Lausanne, CH-1015 Lausanne, Switzerland

(Received 14 May 1993; accepted 6 November 1993)

MoS_x lubricating thin films were deposited by nonreactive, reactive, and low energy ion-assisted radio-frequency (rf) magnetron sputtering from a MoS_2 target. Depending on the total and reactive gas pressures, the film composition ranges between $MoS_{0.7}$ and $MoS_{2.8}$. A low working pressure was found to have effects similar to those of low-energy ion irradiation. Films deposited at high pressure have (002) planes preferentially perpendicular to the substrate, whereas films deposited at low pressure or under low-energy ion irradiation have (002) mainly parallel to it. Parallel films are sulfur deficient ($MoS_{1.2-1.4}$). Their growth is explained in terms of an increased reactivity of the basal surfaces, itself a consequence of the creation of surface defects due to ion irradiation. The films exhibit a lubricating character for all compositions above $MoS_{1.2}$. The longest lifetime in ball-on-disk wear test was found for $MoS_{1.5}$.

I. INTRODUCTION

The lubricating properties of MoS_2 are usually explained by its particular physico-chemical properties.[1] The crystal structure is built by a stacking of S–Mo–S triple layers. Within the layers, the bonding is strong and prominently covalent, while the S external surfaces are weakly reactive. This allows easy crystal bending and easy sliding on the basal surface.

MoS_2 lubricating thin films have been used for several years for lubrication in vacuum environments. Good performances include a low friction coefficient and a long sliding lifetime. They rely on the intrinsic, microscopic properties of the material, but also on macroscopic parameters like film density, orientation, and morphology.

MoS_2 single crystals usually grow in the form of platelets having their largest extension along directions perpendicular to the **c** axis. Since the probability of adsorption on a S basal surface is extremely low, the growth primarily occurs at edge sites in directions normal to **c**. The growth along the **c** direction is mostly due to screw dislocations.

Due to the strong anisotropy of the structure and shape of MoS_2 crystals, crystalline orientation has emerged for several years as a key parameter influencing the mechanical behavior as well as the chemical stability of MoS_2 thin films. From both points of view, films with basal planes parallel with the substrate (thereafter referred to as *parallel films*) are preferred.

Sputtered parallel MoS_2 films have already been obtained by different means. Buck showed that the deposition in an inert plasma, with an extremely low water partial pressure, lead to the formation of stoichiometric MoS_2 thin films with basal planes parallel with the substrate.[2,3] However, this condition on atmosphere and target compositions is so severe that, to our knowledge, nobody was able to reproduce this important result. In a previous work, we showed that, in usual sputtering conditions, there exists a 5–10 nm thick layer at the interface, in which the basal planes are parallel with the substrate. Further growth results in a change in orientation of 90 deg, and in the well-known lamellar morphology.[4] In a recent paper, Hilton reports on the use of this property to build well oriented MoS_2/soft metal/MoS_2... multilayer structures.[5] Another method was used by Aubert *et al.*, who deposited MoS_x from a metallic Mo target in a reactive atmosphere containing H_2S. Depending on the film composition, these authors found a (001) or a (110) texture, i.e., a parallel or perpendicular orientation of the basal planes.

This work follows a similar approach. MoS_x films are deposited from a MoS_2 target. Ion irradiation on the film during growth and preferential resputtering lead to the reduction of the sulfur/molybdenum concentration ratio. Inversely, the sulfur content is increased by the deposition in a reactive atmosphere. Low energy ion irradiation is applied to the growing films by varying the working pressure and thus the plasma and floating potentials,[6–9] or by using a 100 eV Ar^+ ion source. Simultaneous application of both irradiation and reactive deposition allows to distinguish between the mechanical and the chemical effects of ion irradiation. The results show a significant influence of the chemical composition (ratio of S and Mo atomic concentrations) on the preferred orientation. Parallel films can be grown in a composition range $MoS_{1.2}$–$MoS_{1.4}$. For higher S contents the films show the usual lamellar morphology. The growth of parallel films is explained by a weakening of the two-dimensional character of the crystal structure due to defects related to sulfur deficiency. The relatively good lubricating properties of such films are in apparent disagreement with the usual explanation of the lubricating properties of MoS_2, based on the only layered character of the structure.

II. EXPERIMENT

MoS_x thin films are deposited by rf magnetron sputtering from a MoS_2 target. Two different chambers are used: (a) a commercial apparatus (Nordiko), equipped with facilities for

 0734-2101/94/12(2)/494/7/$1.00

TABLE I. Main characteristics of IAS and Nordiko deposition chambers.

	IAS	Nordiko
Target	Hot pressed	MoS_2 (commercial)
Power density P_{rf}	10 Wcm^{-2}	5 Wcm^{-2}
Base pressure P_0	10^{-7} Pa	10^{-5} Pa
Substrate holder	Grounded	Floating
Facilities	Ion source	Reactive sputtering

reactive deposition, and (b) a home-made apparatus (thereafter referred to as "IAS") containing a 3 cm Kaufmann ion source producing a 100 eV Ar^+ oblique ion beam (67° from substrate normal) directed at the growing film. The detailed characteristics of these two reactors are listed in Table I. The substrates are Si[100] wafers for structural and chemical analysis, and polished 440C steel disks for tribological tests.

The structural analysis of the films consists in transmission and scanning electron microscopy (TEM and SEM), and x-ray diffraction (XRD). TEM observations are performed at 300 kV, on cross-sectional samples prepared by mechanical polishing and ion milling. For x-ray diffractometry, we use the θ-2θ geometry, in which the diffracting lattice planes are parallel with the plane of the substrate. The radiation is Cu K_α.

The chemical analysis is performed using Rutherford backscattering spectrometry (RBS) or electron probe microanalysis (EPMA). The RBS measurements have been described elsewhere.[10] The electron microprobe experiments must be carried out to account for the limited film thickness. This requirement is met by using a 5 kV electron beam. It can be shown[11] that, at this energy, the excitation depth of S K_α and Mo L_β lines in MoS_2 are only, respectively, 140 and 130 nm. A 500 nm thick MoS_2 film can thus be considered as a semi-infinite medium. As standards we use natural molybdenite for Mo and S, graphite for C, and an uncoated substrate for Si. Usually, the apparent Si concentration in the film is of the order of one percent. Simulations were performed with program STRATA,[12] based on the model of Pouchou *et al.*;[13,14] they confirmed further that the film thickness was sufficient for carrying safe measurements. They indicated that the weak Si signal from the substrate was due to fluorescence effects.

The tribological characterization is performed using a CSEM[15] ball-on-disk tribometer in dry air, with a 6 mm diameter steel ball and a 5 N normal load.[10]

III. RESULTS

A. Depositions with variable pressure

We present here the characteristics of films grown in pure Ar and without assistance of an ion source. These films are of three different types. Their x-ray diffraction spectra, cross-sectional high-resolution TEM micrographs, and SEM surface views are shown in Figs. 1(a), 2, and 3(a), respectively.

(a) At high Ar pressure ("HP" films, typical composition $MoS_{1.8}$), the films are crystalline and have a lamellar morphology, including many voids. The orientation of basal planes is preferentially perpendicular to the substrate, except

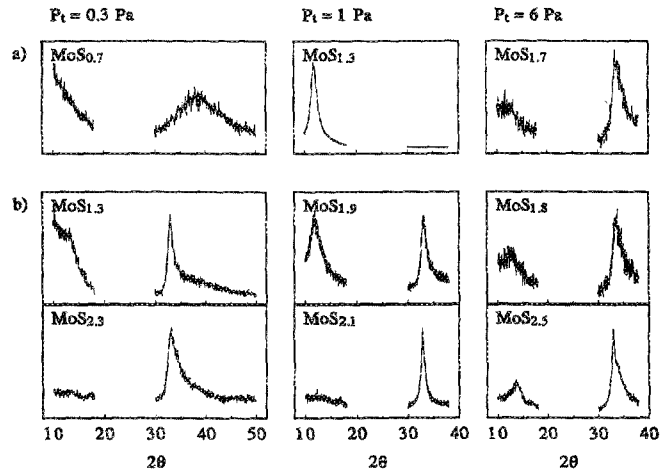

FIG. 1. MoS_x thin films, x-ray diffraction spectra. Films deposited: (a) in pure argon, and (b) in a reactive H_2S/Ar atmosphere, for different values of total working pressure P_t.

in the first 5 nm near the interface, where they are parallel with it. The change in orientation between these two regions is related to a branching process during growth.[4] The crystallite thickness along the **c** direction is $t_c \simeq 5$ nm in the whole film. The diffraction spectrum [Fig. 1(a)] shows two peaks: (002), at $2\theta \approx 13.5°$, and (100), at $2\theta \simeq 33°$. The (002) peak is mainly due to the 5 nm thick interface layer, whereas the (100) peak is due to the upper part of the film.[16] The SEM surface view [Fig. 3(c)] shows a rough surface due to the growth of thin lamellae perpendicular to the substrate.

(b) At low Ar pressure ("LP" films, typical composition $MoS_{1.4}$), the films are dense. The basal planes are mainly parallel with the substrate throughout the whole film. In the diffraction spectrum, this strong preferred orientation leads to an extremely weak (100) peak. The crystallite thickness t_c, determined from TEM micrographs, is much higher than in HP films, and can reach more than 30 nm. This increase in the value of t_c is apparently not consistent with the measurement of the (002) diffraction peak width, which yields approximately the same value as for HP films. Careful obser-

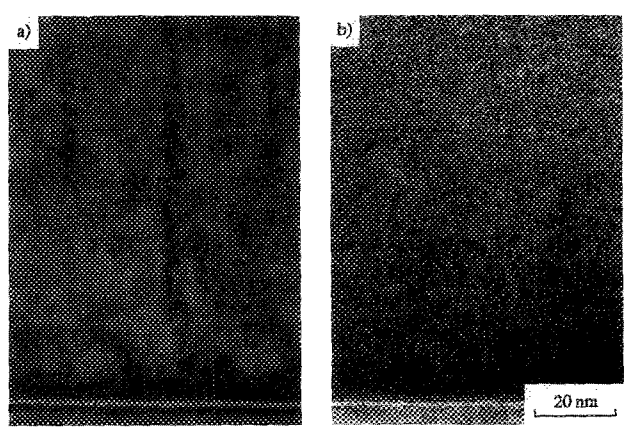

FIG. 2. MoS_x thin films of types (a) HP and (b) LP, high-resolution TEM cross-sectional micrographs.

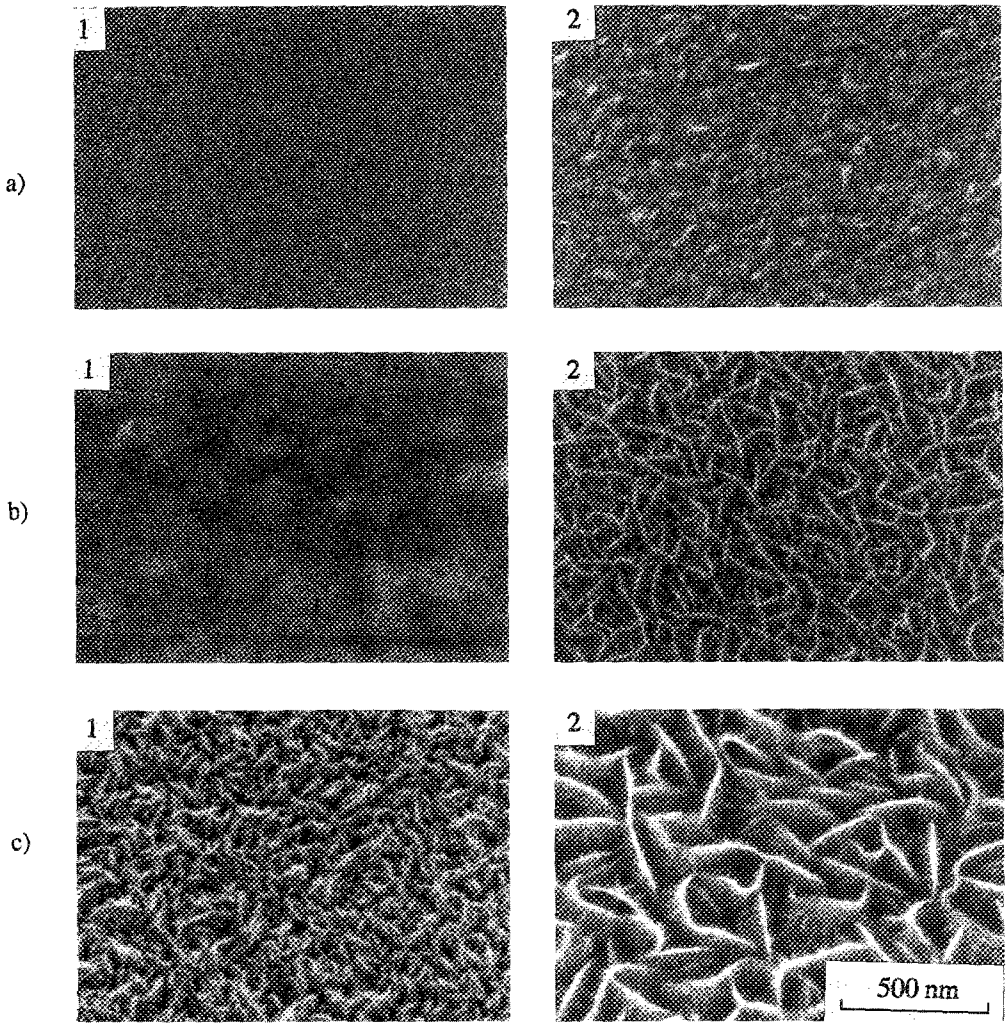

FIG. 3. MoS_x thin films, surface morphologies (SEM plane view). Films deposited at different values of working pressure P_t: (a) 0.3 Pa, (b) 1 Pa, and (c) 6 Pa. The H_2S partial pressure and chemical compositions were: (a1) 0 Pa, $MoS_{0.7}$ (VLP); (a2) 3×10^{-2} Pa, $MoS_{2.3}$; (b1) 0 Pa, $MoS_{1.2}$ (LP); (b2) 3×10^{-2} Pa, $MoS_{2.1}$; (c1) 0 Pa, $MoS_{1.7}$ (HP); and (c2) 2×10^{-1} Pa, $MoS_{2.5}$.

vation of the TEM micrograph [Fig. 2(b)] suggests that the high degree of crystalline disorder in the film is, rather than the grain size, the real reason for the widening of the diffraction peak.

(c) At very low Ar pressure ("VLP" films, typical composition $MoS_{0.7}$), the films are uniformly amorphous and dense. Their surface is so smooth that no contrast at all is observed in the SEM micrographs.

The deposition parameters leading to the growth of these three kinds of films in both deposition chambers are presented in Table II. The substrate temperature was set so as to obtain crystalline films. Its exact value was shown to have little influence on the microstructure of HP films, and no influence on their orientation, provided it was comprised between 100 °C and 500 °C. The same applies to the sputtering power.[17]

TABLE II. Deposition parameters for HP, LP, and VLP films. T_s: substrate temperature, P_{Ar}: argon pressure, and d_{cs}: distance between substrate and target.

		T_s (°C)	P_{Ar} (Pa)	d_{cs} (mm)
HP	IAS	300	2.2	95
	Nordiko	100	6	80
LP	IAS	300	0.4	95
	Nordiko	100	1	80
VLP	Nordiko	100	0.3	50

The main effect of the deposition pressure is to modify the flux and energy of particles incident on the substrate during film growth. A low working pressure tends to increase the positive plasma potential V_p. In addition, if the substrate holder is insulated, or if the substrate itself is an insulator, the different values of electron and ion flux at the substrate, due to the different masses and temperatures of these particles, generate a negative floating potential V_f at the surface of the substrate. The effect of the potential difference between the plasma and the substrate ($\Delta V = V_p$ or $\Delta V = V_p - V_f$) is to accelerate positive ions from the plasma onto the growing film.[6-9] In the case of MoS_2, a consequence of this ion irradiation is the preferential resputtering of S atoms,[18-20] leading to the creation of sulfur vacancies on the basal surface.

This mechanism provides a consistent explanation for our results. The sulfur content in our films decreases strongly with decreasing Ar pressure. When the substrate is electrically insulated (Nordiko chamber), the nonzero floating potential contributes to ΔV, the corresponding sulfur loss is more severe, and the working pressure required to reach a

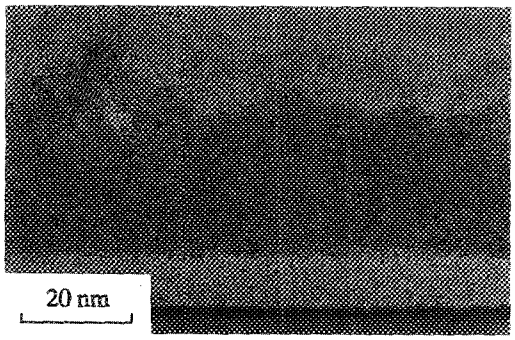

FIG. 4. MoS_2 film deposited at high pressure in 16 alternating deposition/irradiation/··· cycles of 10 s each. Cross section observed by high-resolution TEM. The interfacial parallel layer is significantly thicker than in normal HP films [Fig. 2(a)].

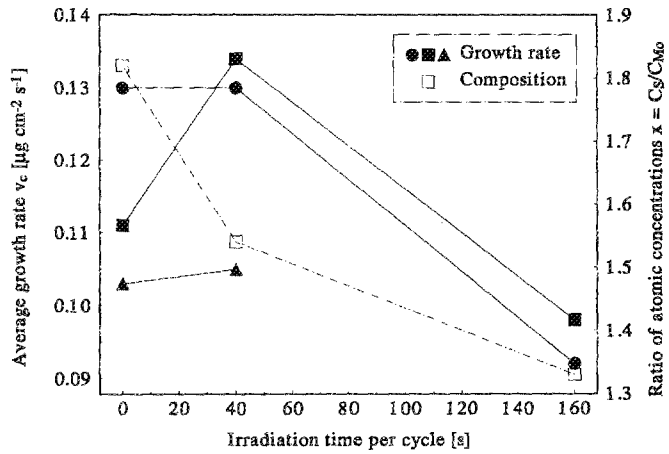

FIG. 5. MoS_x thin films grown in alternating deposition/irradiation cycles: composition and average growth rate as a function of the irradiation time τ_i. The deposition time τ_d is 40 s. The lines join data from one same series of samples.

given composition is accordingly higher than when the substrate is grounded (see Table II).

The short substrate-to-target distance used for VLP films was intended to provide a lesser thermalization of the sputtered species. Energetic condensing atoms are expected to have an effect similar to that of impinging ions, thus enhancing the global effect of a low deposition pressure.

B. Direct ion irradiation

Low energy ion irradiation is applied to a film growing at high pressure (HP). The working pressure of the gun is two orders of magnitude lower than that of the sputtering source. the process is therefore carried out in several deposition/irradiation/··· cycles, with deposition times τ_d and irradiation times τ_i. The deposition time τ_d is 40 s and corresponds to an effective thickness of 9 nm at the density of bulk MoS_2. The beam energy is 100 eV and the beam current is 5 mA. It has already been shown that, at moderate irradiation doses, this process results in an alignment of the basal planes with the incidence direction of the beam,[21,22] while the lamellar morphology is conserved. At high doses, one observes the disappearance of the lamellar morphology. A TEM cross section shows a significant increase in thickness of the interfacial layer in which the basal planes are parallel with the substrate (Fig. 4).

For given values of τ_d, the ratio x of S and Mo atomic concentrations strongly decreases with increasing irradiation time τ_i, as shown on Fig. 5. Whereas the deposition phases are characterized by a *deposition rate*, the complete deposition/irradiation/··· cycle is described by an *average growth rate*,defined as $v_c = m_s/\tau_d$, where m_s is the total film mass per unit surface after the full process m_s is determined by direct weight measurement, or from the effective thickness used for the calculation of the RBS spectra. The evolution of v_c as a function of the irradiation time is reported on Fig. 5. For high doses, the average growth rate decreases. One would expect the same behavior, though to a lesser extent, for low irradiation doses. This is clearly not the case, since v_c actually experiences a small increase for $\tau_i = 40$ s.

The simultaneous decrease in sulfur concentration and increase in average growth rate indicates on the one hand the presence of resputtering, and, on the other hand, an increased surface reactivity, strong enough to compensate the loss of material due to resputtering. The increased thickness of the parallel interfacial layer (Fig. 4) suggests that the probability of adsorption on the basal surfaces is increased by irradiation, leading to an enhanced growth velocity in the **c** direction.

C. Reactive deposition

We have shown that low energy ion irradiation during film deposition promotes grain growth in the **c** direction, and leads to the formation of parallel films. These films are strongly sulfur deficient. The question arises whether it is possible to grow stoichiometric and parallel films by combining ion irradiation and reactive deposition to compensate for the loss due to the preferential resputtering.

For this purpose, films are deposited in the presence of a gas mixture containing H_2S and Ar. The total pressure P_t is kept constant, while the H_2S partial pressure, P_{H_2S}, is varied. The experiment is carried out for three different values of P_t, each corresponding to one of the three previously described types of films, i.e., HP, LP, and VLP.

The effect of H_2S on film composition is shown in Fig. 6. For $P_t = 0.3$ Pa and $P_t = 1$ Pa, the ratio x is limited by a minimum value, corresponding to the composition in the absence of reactive gas, and by a maximum value corresponding to a saturation. Whereas the minimum x is lower at 0.3 Pa than at 1 Pa, its maximum value is higher at 0.3 Pa than at 1 Pa. At $P_t = 1$ Pa, the transition between the two end compositions extends over two orders of magnitude of H_2S partial pressure, around a central value of 10^{-3} Pa; it is much steeper at very low total pressure. The behavior is different at $P_t = 6$ Pa: the composition, of the order of $x = 1.7$, remains unchanged for H_2S partial pressures below 10^{-2} Pa. Above, the ratio strongly increases to reach a maximum value of $x \simeq 2.8$ for $P_{H_2S} = 5 \times 10^{-1}$ Pa. No saturation appears in the range of partial pressures investigated here.

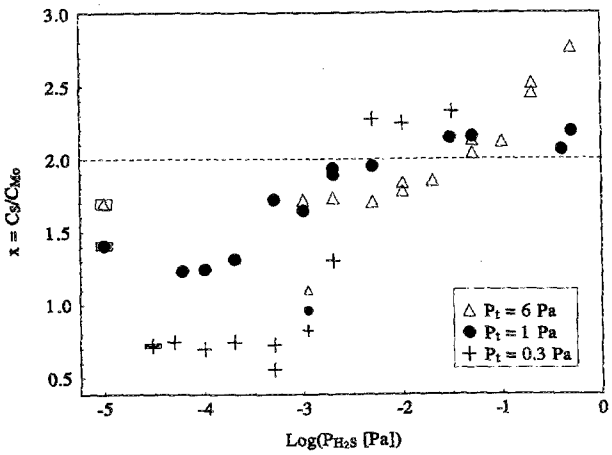

FIG. 6. MoS_x thin films deposited in a reactive atmosphere: ratio of atomic concentrations as a function of the H_2S partial pressure, for various values of the total working pressure P_t.

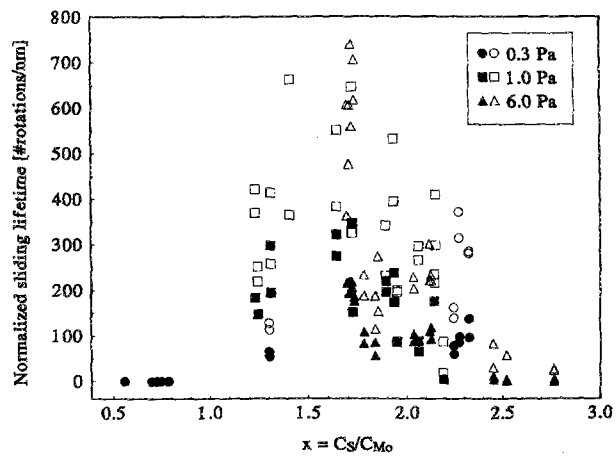

FIG. 7. Reactively sputtered MoS_x films: sliding lifetime, divided by film thickness, as a function of the concentration ratio $x=C_S/C_{Mo}$, for different values of the total working pressure P_t. White symbols: total lifetime (μ <0.3); black symbols: end of the steady state sliding regime.

At 10^{-3} Pa, which is the order of magnitude of P_{H_2S} necessary to modify the composition of films deposited at low and very low P_t, the mean free path Λ of the sputtered species with respect to collisions with H_2S is much larger than the separation between the target and the substrate, d_{cs}.[6] At high P_t, the increase in sulfur contents begins at higher P_{H_2S}, of the order of 10^{-2} Pa. In this pressure range, Λ and d_{cs} become comparable. We suggest two different mechanisms for the sulfuration of MoS_x films deposited at low and very low P_t and those deposited at high P_t. In the first case, the reaction takes place at the film surface, and is activated by ion irradiation. In the second case, at high pressure, the reaction occurs during gas phase collisions, and leads to the deposition of MoS_x groups formed after collisions between Mo atoms and H_2S molecules, in addition to isolated, as-sputtered S and Mo atoms. This last mechanism can account for the very high sulfur content of films reactively sputtered at high working pressure.

The XRD spectra and the surface morphologies of reactively sputtered films are presented on Figs. 1(b) and 3, respectively.

For films deposited at P_t=0.3 Pa, the increase in sulfur content comes together with a crystallization. Thus all the investigated films in the present study, with concentration ratio x larger than 1.2, are crystalline. The preferred orientation is (002) $\perp$ substrate. TEM observations have shown that the absence of the (002) peak in some samples is due to the presence of an amorphous near-interface layer instead of the usual crystalline, parallel layer. The surface morphology tends to become coarser with increasing x, though no lamellar morphology is observed.

For films deposited at P_t=6 Pa, the diffraction spectrum is not significantly modified by reactive deposition. Nevertheless, the SEM surface micrographs indicate a considerable increase in the length of the lamellae, their thickness, however, remaining approximately constant.

The most striking effect of reactive deposition appears for P_t=1 Pa. The film structure, which is originally of LP type, turns to HP type when x exceeds 1.4. This is shown by the presence of a (100) peak in the diffraction spectrum [for $x>1.5$, Fig. 1(b)], and by the lamellar morphology observed by SEM [for $x\geq 2.0$, Fig. 3(b)].

D. Tribological properties

Ball-on-disk friction measurements on MoS_x films reveal, after the run-in step, two distinct main regimes: During the first part of the test, the measured friction force is approximately constant. The friction coefficient remains below 0.05 for all films. We call this regime *steady state sliding*. At a further stage, the friction coefficient shows sharp peaks and oscillations, taking values ranging from the steady state sliding value to 0.3. For evaluation of the sliding lifetime, we consider then two criteria. The first one is the end of the steady state sliding regime; the second one is the final wear of the film, and is defined as the time when the friction coefficient reaches 0.3.

Figure 7 shows the sliding lifetime of films deposited at different values of total working pressure P_t, as a function of their concentrations ratio x. The VLP films ($x<0.8$) are not lubricating at all. The sulfur rich films ($x>2.5$) have a very short lifetime. The best properties are achieved for $x\simeq 1.5$. There is no direct influence of P_t on the tribological behavior of the films.

IV. DISCUSSION

The comparison of results from film growth at different working pressures and from ion beam assisted deposition shows strong effects of ion irradiation on film structure and composition. A purely chemical effect is the preferential resputtering of sulfur atoms from the films, which allows growth of films in a wide range of under stoichiometric compositions. A purely structural effect, on the other hand, can be observed on Fig. 3 between films of similar compositions but different deposition pressures: The samples deposited at lower pressure (i.e., under stronger irradiation) have a markedly smoother surface and denser morphology. The most striking structural effect of this irradiation is the modification

of the preferential crystal orientation, from (002) ⊥ substrate, in the absence of irradiation, to (002) ∥ substrate, under moderate irradiation. Films having this last orientation are characterized by a larger grain size in the c direction, t_{uc}, than lamellar films. In other words, whereas in lamellar films the crystallites have a shape similar to that of molybdenite single crystals, characterized by a wide extension in the plane perpendicular to c, in parallel films they have a rather prismatic shape, with sizes of the same order in all crystal directions. Moderate irradiation doses increase the average crystal growth rate (cf. Fig. 5). It can be interpreted as the result of an increase in the reactivity of the basal plane, via creation of sulfur vacancies. The attempt to grow sulfur-rich parallel films by reactive sputtering failed, clearly indicating a close relationship between crystallite shape and sulfur concentration. Such an effect has been observed in another transition metal dichalcogenide, titanium sulfide.[23] Where as TiS_2 crystals are lamellar in shape, like MoS_2 crystals, $TiS_{1.7}$ are prismatic, and elongated along their c direction. The structure of $TiS_{1.7}$ includes many polytypes, but primarily consists of a TiS_2 structure with additional Ti atoms in the gap between S planes. The prismatic crystal shape is thus a consequence of a weakening of the two-dimensional character of the crystal.

The relationship between crystal shape and preferential orientation in the film can be explained by the following model. Under weak irradiation, the basal surface of MoS_x crystallites is considered as inert, like in bulk MoS_2 crystals. Atoms condensing on the growing film cannot easily find an energetically favorable site on the basal surface. Thus they have a high probability of being resputtered or desorbed. The only reactive sites available are edge sites, which are found either at steps on the basal surfaces, or, more often, on the ($hk0$) surfaces of crystallites growing from branching sites. These last crystallites can then reach very large sizes, leading to the lamellar morphology. Under moderate irradiation, defects are created on the basal surfaces. Exposing dangling bonds. These surfaces become more reactive, incident atoms can more easily find favorable sites, and the growth in the c direction is promoted. The growth velocity of crystals with (002) ∥ substrate is then comparable to that of perpendicular crystallites originating from branching sites, and the parallel preferred orientation is conserved throughout the films.

Since the growth of parallel films relies on an increased reactivity of the basal surfaces, related to the presence of defects (S vacancies, Mo interstitials or substitutionals, for example), the films do not strictly fulfill the condition of perfect saturation of the covalent bonding within the S–Mo–S layers. Due to inhomogeneities in the spatial distribution of defects, defect-free areas may, however, exist, with locally weak interplane bonding. The origin of the good lubricating properties of MoS_x coatings results therefore from more than just the layered crystal structure. It has actually been shown that lubrication in MoS_x thin films involves complex intercrystallite displacements.[10] The deformation of the individual grains, with possible slip of dislocations, work hardening, etc., as well as their collective behavior, should be considered further.

V. CONCLUSION

MoS_x thin films were deposited at various total working pressures, including variable amounts of H_2S reactive gas. Low working pressure is known to increase the intensity of film irradiation by energetic particles. In addition, the effects of low pressure and ion irradiation were shown to be similar by submitting films deposited at high pressure to irradiation by a 100 eV ion beam.

The consequences of a strong irradiation are a low sulfur content (down to $MoS_{0.7}$) due to preferential resputtering, and a densified morphology. Addition of reactive gas in the plasma can increase the sulfur content up to overstoichiometric concentrations ($MoS_{2.8}$), and leads to more open morphologies. The reactivity of the film surface with H_2S appears to be promoted by ion irradiation.

Within a range of understoichiometric values of sulfur concentration ($MoS_{1.2\text{-}1.4}$), the reactivity of the basal surface, and thus the crystal growth velocity in the c direction, are increased, leading to the growth of thick crystallites, forming films with basal planes preferentially parallel with the substrate. For S concentrations above $MoS_{1.4}$, the crystal growth velocity in the c direction is low, like in MoS_2 crystals. Though at the interface the basal planes are parallel with the substrate, the preferred orientation turns to become perpendicular to the substrate in the upper part of the film. Below $MoS_{1.0}$, the films are amorphous.

All films with composition over $MoS_{1.2}$ exhibited lubricating properties, with a friction coefficient below 0.05. The best endurances were found for compositions close to $MoS_{1.5}$, regardless of the total and H_2S working pressure.

ACKNOWLEDGMENTS

This work has been supported by the Fondation Suisse pour la Recherche en Microtechnique and by the Fonds National Suisse pour la Recherche Scientifique. The depositions were carried out by G. F. Clerc and H. Jotterand. The RBS measurements were performed at the University of Neuchâtel by Dr. J. Weber.

[1] P. D. Fleischauer, Thin Solid Films **154**, 309 (1987).
[2] V. Buck, Thin Solid Films **139**, 157 (1986).
[3] V. Buck, Wear **114**, 263 (1987).
[4] J. Moser and F. Lévy, J. Mater. Res. **7**, 734 (1992).
[5] M. R. Hilton, R. Bauer, S. V. Didziulis, M. T. Dugger, J. M. Keem, and J. Scholhamer, Surf. Coat. Technol. **53**, 13 (1992).
[6] B. Chapman, *Glow Discharge Process* (Wiley, New York, 1980).
[7] J. L. Vossen and W. Kern, *Thin Films Processes* (Academic, New York, 1978).
[8] R. Meisser, A. P. Giri, and R. A. Roy, J. Vac. Sci. Technol. A **2**, 500 (1984).
[9] R. Luthier, "Propriétés structurales et optiques de couches minces composites déposées par pulvérisation cathodique," EPFL - thèse No. 849, Lausanne (1990).
[10] J. Moser and F. Lévy, J. Mater. Res. **8**, 206 (1993).
[11] J. I. Goldstein, D. E. Newbury, P. Echlin, D. C. Joy, C. Fiori, and E. Lifshin, *Scanning Electron Microscopy and X-Ray Microanalysis* (Plenum, New York, 1981).
[12] *SAMx STRATA Manual*, SAMx, 78280 Guyancourt, France (1992).
[13] J. L. Pouchou, F. Pichoir, and D. Boivin, Microbeam Analysis 120 (1990).
[14] J. L. Pouchou and F. Pichoir, Scanning **12**, 212 (1990).

[15]Centre Suisse d'Electronique et de Microtechnique, Neuchâtel, Switzerland.
[16]J. Moser, H. Liao, and F. Lévy, J. Phys. D: Appl. Phys. **23**, 624 (1990).
[17]J. Moser, H. Liao, and F. Lévy, 10th International Conference on Vacuum Metallurgy Proceedings, Vol. 2 Metallurgical Coatings, Beijing, 1991 (unpublished), pp. 157–165.
[18]J. R. Lince, D. J. Carré, and P. D. Fleischauer, Langmuir **2**, 805 (1986).
[19]J. R. Lince and P. D. Fleischauer, J. Vac. Sci. Technol. A **5**, 1312 (1987).
[20]J. R. Lince, T. B. Stewart, M. M. Hills, and P. D. Fleischauer, Surf. Sci. **210**, 387 (1989).
[21]P. Gribi, Z. W. Sun, and F. Lévy, J. Phys. D: Appl. Phys. **22**, 238 (1989).
[22]F. Lévy, P. Gribi, Z. W. Sun, and Ph. Schmid, 7th International Conference Ion and Plasma Assisted Techniques Proceedings, Geneva, 1989 (unpublished), pp. 274–279.
[23]J.-J. Legendre, R. Moret, E. Tronc, and M. Huber, J. Appl. Cryst. **8**, 603 (1975).